Published in final edited form as:
Proteomics. 2008 April ; 8(7): 1384–1397. doi:10.1002/pmic.200700787.

Comparative Glycomics of Connective Tissue Glycosaminoglycans

Alicia M. Hitchcock[1], **Karen E. Yates**[2], **Catherine E. Costello**[1], and **Joseph Zaia**[1]

1 *Department of Biochemistry, Boston University School of Medicine, Boston, MA 02118*

2 *Brigham and Women's Hospital and Harvard Medical School, Department of Orthopedic Surgery, Boston, MA 02115*

Abstract

Homeostasis of connective joint tissues depends on the maintenance of an extracellular matrix, consisting of an integrated assembly of collagens, glycoproteins, proteoglycans and glycosaminoglycans (GAGs). Isomeric chondroitin sulfate (CS) glycoforms differing in position and degree of sulfation and uronic acid epimerization play specific and distinct functional roles during development and disease onset. This work profiles the CS epitopes expressed by different joint tissues as a function of age and osteoarthritis. Glycosaminoglycans were extracted from joint tissues (cartilage, tendon, ligment, muscle and synovium) and partially depolymerized using chondroitinase enzymes. The oligosaccharide products were differentially stable isotope labeled by reductive amination using 2-anthranilic acid- d_0 or -d_4 and subjected to amide-HILIC on-line liquid chromatography-tandem mass spectrometry. The analysis presented herein enables simultaneous profiling of the expression of non-reducing end, linker region, and Δ-unsaturated interior oligosaccharide domains of the CS chains among the different joint tissues. The results provide important new information on the changes to the expression of CS GAG chains during disease and development.

Keywords

Glycosaminoglycan; connective tissue; mass spectrometry; chondroitin sulfate; glycomics

1. Introduction

The biological activities of chondroitin/dermatan sulfate (CS/DS) glycosaminoglycans (GAGs) arise from a series of non-template driven biosynthetic events [1]. Sulfation and epimerization reactions occur with polymerization of the CS/DS chains and the mature structures depend on the activities of the biosynthetic enzymes, the levels of which are under complex control. In addition, the targeted compartment of the core protein (membrane bound or secreted) and the number and density of GAG chains influence the manner in which the nascent proteoglycan travels through the Golgi network and the structure of the CS/DS chains [2,3]. Variation of structures of GAGs on the cell surface and in the extracellular matrix (ECM) may be viewed as a means of elaborating cellular responses to growth conditions using a finite number of core proteins. Because the activity levels of the biosynthetic enzymes differ among tissues and over time [4], the structures and functions of CS/DS chains vary spatially and temporally in connective tissues [5].

Address correspondence to: Joseph Zaia, Department of Biochemistry, Boston University School of Medicine, MS Resource, 670 Albany St., Boston, MA 02118. Telephone: (617)-638-6762. Fax: (617)-638-6760. Email: jzaia@bu.edu.

Joint tissue integrity depends on a variety of specific and organized interactions between the ECM and the cells that regulate tissue homeostasis. Proteoglycans, specifically aggrecan, are major components of the ECM of joint tissue and provide many of their characteristic physical and chemical properties. In particular, CS chains provide swelling properties that are key to resistance to compressive forces on the tissue [6]. Aggrecan contains approximately 100 CS chains per molecule [7]. CS/DS consists of repeating disaccharide units of (4Hexβ/α1-3GalNAcβ1-) polymerized in chains of size varying from 20 to 50 kDa depending on the core protein, tissue location, age and disease contexts. The chains consist of mixtures of domains with high or low iduronic acid (IdoA) content with differing patterns of sulfation for aggrecan [8].

GAG chains may be viewed as composed of three regions: the non-reducing end, the interior, and the reducing end linker. The linker tetrasaccharide for both CS/DS and heparin/heparan sulfate (HS) chains consists of (GlcAβ1-3Galβ1-3Galβ1-4Xylβ1-O-Ser). For CS/DS GAGs, sulfation may exist at either the 4- or 6-positions of the next to last GalNAc, the 4- or 6-positions of the Gal residues and may be phosphorylated at the 2-position of Xyl [9–14]. The GlcA residue may be epimerized to IdoA in DS chains [15,16]. These modifications may play roles in the regulation of CS/DS versus HS chain elongation during GAG biosynthesis. Lyase digestion of CS/DS chains produces linker tetra- and hexasaccharides that contain a 4,5-unsaturated (Δ-unsaturated) HexA residue.

The internal disaccharides are divided into domains of differing sulfation and epimerization levels, the patterns and extents of which depend on the tissue location. The composition of the internal domain is often measured on the basis of disaccharides produced from lyase digestion. CS/DS chains play roles in the regulation of axonal outgrowth and neuronal path finding [17]. Such activity depends on the presence of over-sulfated domains of the D- and E-types that are known to exist in brain tissue [18]. The pattern of CS/DS chain sulfation changes from predominantly 4-sulfation to increased levels of 2-, and 6-sulfation with the presence of 4,6-sulfation resulting from brain injury and subsequent glial scar formation [18]. In addition, pathogens including malaria parasites [19–21] and the *Borrelia burgdorferi* spirochete, herpes simplex I virus [22], recognize cell surface CD/DS, and their binding is dependent on the sulfation pattern.

For cartilage aggrecan, alterations in GAG compositions, such as changes in sulfation pattern, have been correlated not only with development and aging, but also with osteoarthritis (OA) [23–26]. Previous research has produced evidence suggesting isomeric CS/DS glycoforms differing in position and degree of sulfation play specific and distinct functional roles during development and disease onset [27–29]. Mature OA cartilage has been shown to consist primarily of 6-*O*-sulfated CS, while juvenile cartilage contains a mixture of 4- and 6-*O*-sulfated CS [23,27,30,31]. Osteoarthritic cartilage displays a sulfation pattern similar to that observed for adolescent individuals, possibly resulting from changes to chondrocyte phenotype in an attempt to repair tissue damage.

Biosynthetic data show that CS/DS chains do not contain a distinct non-reducing terminal residue [1]. Rather, the structure of this residue results from specific enzymatic activities, the levels of which vary spatially and temporally [25,32]. For juvenile cartilage (age 0–15 years) CS/DS chains, the most abundant non-reducing end structure is GalNAc4S with lower abundances of GlcAβ1-3GalNAc4S, and GlcAβ1-3GalNAc6S. In adults (age 22–72 years), approximately half of chains terminate in GalNAc4,6S [32], and this level diminishes in OA cartilage [25]. Sulfation of the non-reducing terminal GalNAc residue occurs by the activity of specific sulfotransferases, whose activities do not depend on the structure of the adjacent disaccharide [33]. Such non-reducing end structures are believed to be the most accessible parts of GAG chains with respect to interaction with binding partners. Analytical limitations

have made it difficult to extend these observations to longer oligosaccharides containing the non-reducing end.

The structures of GAGs in other connective tissues are known in less detail. The two predominant proteoglycans found in both tendon and ligament are decorin and biglycan [34]. The total GAG content present in tendon and ligament is known to be small, with the majority of the GAG content being composed of hyaluronan, followed by DS, and small amounts of CS [35]. The major GAG content of muscle tissue can vary, based on species, age and source [36]. In mouse muscle tissue, hyaluronan and DS were reported to make up the majority of the GAG composition, with small amounts of CS and HS also present [36]. Dermatan sulfate was found to make up the major contribution of sulfated GAGs in both rabbit muscle [37] and porcine skeletal muscle [38].

In order to develop a better understanding of the roles of GAG expression during development, homeostasis and disease states, an improved analytical system is needed. Such a system must make rapid, precise, and sensitive comparisons in the expression of GAG chains among different tissue samples. It must produce data on sulfation and epimerization of the extended GAG oligosaccharides that are most functionally relevant in terms of potential for interaction with protein partners. In this work, a liquid chromatography-mass spectrometry approach is described to meet this need.

The region from which lyase digestion products of CS/DS GAGs derive may be assigned based on their mass values. Each mass defines a monosaccharide composition that indicates whether the oligosaccharide was produced from the non-reducing end, the internal, or the reducing end linker region. Each composition consists of a mixture of sulfation position and uronic acid epimerization isomers. Tandem mass spectrometry is an effective means for determining mixture percentage of such isomers with respect to sulfation and epimerization [31,39]. In order to make precise comparisons among a series of biological samples, differential stable isotope labeling by reductive amination may be used. Pairs of samples may then be mixed and analyzed simultaneously, facilitating quantitative analysis. All tissue-derived CS samples are measured against the same reference mixture, labeled with the light form of a reductive amination tag.

This paper demonstrates whole chain analysis for profiling CS/DS GAG expression as a function of spatial location in the joint (cartilage, tendon, ligament, muscle and synovial tissue). In addition, whole CS/DS chain analysis is shown for cartilage tissue as a function of age and disease state. This work employs a robust, MS-compatible extraction procedure that is applicable to all joint tissues. Whole GAG chain profiles were generated using a novel capillary hydrophilic interaction chromatography (HILIC)-mass spectrometry system. The MS dimension determines changes to the compositions of CS GAG oligosaccharides among the different joint tissues. The tandem MS dimension determines changes to the positions of sulfation and epimerization of selected oligosaccharides. The data serve to compare the expression of and non-reducing end, internal, and linker region structures simultaneously.

2. Materials and methods

Materials

CS type A (GlcA, GalNAc-4-sulfate), CSB (IdoA, GalNAc-4-sulfate) CSC (GlcA, GalNAc-6-sulfate), and chondroitinase ABC, B and AC1 were obtained from Seikagaku America/Associates of Cape Cod (Falmouth, MA). 2-Anthranilic acid (d_0-2AA) was purchased from Fluka Chemika (Buchs, Switzerland), sodium cyanoborohydride and sodium borohydride were from Aldrich Chemicals Co. (St. Louis, MO), and 2-anthranilic-3,4,5,6-d_4 acid (d_4-2AA) was from C/D/N Isotopes (Quebec, Canada). Cellulose packing material Ultra Micro Spin Columns

and strong anion exchange packing material Ultra Micro Spin Columns were purchased from Harvard Apparatus (Holliston, MA). Pepclean C18 reversed phase spin columns were purchased from Pierce (Rockford, IL).

Tissue

Bovine cartilage, muscle, tendon, ligament and synovium were removed from shoulder joints of young calves and adult human cartilage was obtained under an Institutional Review Board-approved protocol for discarded tissue (total knee arthroscopy for osteoarthritis) as described previously [31]. Briefly, for this study, 5 human explants (median weight, 23 mg), ranging in grade from 1–3, were collected from 5 donors (3 men and 2 women, ages 62 – 81). An adaptation of the dimethylmethylene blue (DMMB) assay was used to measure sGAG content [31].

Extraction of GAGs from connective tissue samples

Sulfated GAGs were extracted from connective tissue samples as described previously [31]. Briefly, GAGs were released from the core protein in papain-digested connective tissue samples with a 1.0 M $NaBH_4$, 0.05 M NaOH solution at 45 °C for 16 h. Hydrophobic biomolecules were removed from released cartilage samples via Pepclean C18 spin columns. The sample was dissolved in 50-μL of water and precipitated in 9 volumes of chilled ethanol. Cationic biomolecules were removed from the GAG pellet via strong anion exchange ultra micro spin columns. Cationic biomolecules were washed off with three 100-μL volumes of 50 mM sodium phosphate pH 3.5. The GAG mixture was then eluted with two 100-μL volumes of 1M NaCl, dried *in vacuo* and precipitated in 9 volumes of chilled ethanol.

Preparation of Δ-Unsaturated Chondroitin Sulfate Oligosaccharides

Larger cartilage samples (5-μg by DMMB assay) were partially digested with chondroitinase ABC (3-μL, 4 mU/nμL), chondroitinase AC1 (3-μL, 2 mU/μL), and chondroitinase B (1-μL, 0.5 mU/μL) at 37 °C, to an absorbance value (232 nm) equal to 0.045 for bovine samples and 0.012 for human samples, and boiled for 1 min. This degree of digestion was found to reproducibly depolymerize 5-μg of each respective cartilage sample to 30% reaction completion. Smaller cartilage samples (3-μg and 1-μg by DMMB assay) were partially digested to 30% reaction completion with chondroitinases to an absorbance value (232 nm) equal to 0.027 and 0.009, respectively for juvenile bovine and 0.007 and 0.002, respectively, for adult human samples and boiled for 1 minute. Muscle, ligament, tendon and synovium connective tissues, in 5-μg quantity by DMMB assay, were partially depolymerized under the same conditions described above for 5-μg cartilage tissue samples. Connective tissue samples were digested to an absorbance value (232 nm) equal to 0.213 for muscle, 0.071 for ligament, 0.081 for tendon, and 0.155 for synovium tissue. Partial depolymerization products were dried *in vacuo* for subsequent reductive amination with d_4-2-AA.

Derivatization of Oligosaccharides with d_0- and d_4-2-AA

All oligosaccharides were derivatized with d_0- or d_4-2-AA according to the method of Bigge *et al*. [40]. Briefly, a dried CSA sample (10-μg) was dissolved in 10-μL of a reaction reagent containing d_0-2AA in DMSO/glacial acetic acid (7:3) and 1.0 M sodium cyanoborohydride. All other partially depolymerized 1-μg, 3-μg, and 5-μg cartilage and connective tissue samples were derivatized using d_4-2AA under the same conditions. The glycan solutions were then centrifuged for 3 min and incubated at 65 °C for 3 h. Excess reagents were removed with cellulose ultra microspin columns as described below.

Derivatization Sample Clean-Up

The cellulose column was first hydrated with five 200-μL volumes of water, rinsed with five 200-μL volumes of 30% acetic acid solution, and then with three 200-μL volumes of acetonitrile. The 2-AA derivatized reaction mixture was applied to the column allowing 15 min for it to adsorb to the cellulose. Excess reagents were washed off with three 200-μL volumes of acetonitrile followed by two 200-μL volumes of 96% acetonitrile. The derivatized glycan was then eluted with two 100-μL volumes of water and dried.

Amide-HILIC Chromatography

A nanoscale amide-hydrophilic interaction chromatography (HILIC)-capillary column (250 μm i.d. ×150 mm) was packed in house using a column packing bomb. Resin (5 μm particle size, 80 Å pore size) was removed via syringe pump from a 4.6 mm TSKgel amide-80 guard column (Tosoh Bioscience, Grove City, OH). The amide-80 resin was then packed into the silica capillary (250 μm i.d. ×360 μm o.d.; Polymicro Technologies, Phoenix, AZ) under a pressure of 1500 psi in the presence of 70% ethanol.

LC-MS/MS Analysis

Derivatized glycan samples were purified using size exclusion chromatography (SEC) and dried. Glycan samples were then fractionated using amide-HILIC chromatography with online tandem mass spectrometric detection. The amide-HILIC capillary column was equilibrated as described by Wuhrer et al. [41]. Briefly, the column was equilibrated in 80% solvent A (10% acetonitrile, 0.05 M formic acid solution, pH 4.4) and 20% solvent B (20% solvent A in acetonitrile) at 3 μL/min. The HPLC gradient was pumped at a flow rate of 100 μL/min, and was split prior to the injector; flowing only 3 μL/min into the amide-HILIC column. The eluent from the oligosaccharide mixture (10-μL) was injected directly into the mass spectrometer (MS).

The HPLC system was connected via 50 micron diameter silica capillary tubing to a Bruker Daltonics (Billerica, MA) Esquire 3000 quadrupole ion trap mass spectrometer equipped with a standard electrospray ion source. The spray voltage was set at 3 kV; capillary temperature was set to 250°C; the nebulizer gas (He) was set to 10 psi and the drying gas (N_2) was set to 5 L/min. The capillary exit was set to −50.9 V and the skimmer potential was set to −10 V, so as to prevent in-source fragmentation. The HPLC flow was sent directly into the mass spectrometer at 3 μL/min. All scans were acquired in the negative ion mode using the automated MS^n feature of the ion trap. The instrument was set to cycle between the MS and MS/MS modes until the entire mixture had eluted through the column. The MS/MS scans were summed for the most abundant charge state for the CS oligosaccharides; this corresponded to one negative charge per sulfate group.

Statistical Analysis

Statistical pair-wise comparisons were calculated using Microsoft Excel 2003. A t-test assuming two samples using either equal or unequal variances, depending on the ion abundances of the tissue samples, was applied using the formulas within Excel.

3. Results

Amide-HILIC LC/MS for CS/DS

Amide-silica stationary phase allows retention of polar compounds through hydrophilic interaction (HILIC) and elution using a gradient of increasing water concentration. Amide-silica columns are less basic than amine-silica, and have been used for separation of CS/DS disaccharides [42] and the oligosaccharides [43] produced by lyase digestion. Conditions for

separations of glycans [44] employ a water/acetonitrile gradient with ammonium formate modifier. Similar conditions have been applied to on-line LC/MS of *N*-glycans [45]. Recently, the use of custom-packed capillary amide-80 HILIC columns for LC/MS of *N*-glycans has been demonstrated [41,46].

In this work, amide–HILIC chromatography is applied to separation of CS/DS oligosaccharides with on-line negative ESI MS detection. A 250-μM internal diameter column was operated at 3 μL/min, an approximately ten-fold reduction in flow as compared to the size-exclusion chromatography (SEC) platform used for LC/MS of CS/DS GAGs in previous work [31,39]. The resultant increase in the concentration of analytes entering the MS ion source allows either analysis of 10-fold less material, or increased sensitivity of detection of low abundance oligosaccharides while consuming the same quantity as in the earlier work. Amide–HILIC chromatography enables baseline chromatographic separation of disaccharides Δ(1,1,1) to dodecasaccharides Δ(6,6,6), where oligosaccharide compositions are given as (HexA, GalNAc, SO_3) (X,Y,Z) and Δ signifies 4,5-unsaturation of the non-reducing end HexA residue. The additional degree of separation reduces the extent to which abundant structures suppress ionization of less abundant ones. In addition, the increased sensitivity allows detection of ions corresponding to the reducing end, containing the GAG linker tetrasaccharide, and the non-reducing end, lacking a Δ unsaturation. Thus, it is possible to profile the non-reducing chain structures that are most likely to interact with protein partners, the Δ-unsaturated structures that make up the interior of the parent CS/DS chains, and the reducing end linker region in a single analysis.

Amide-HILIC LC/MS of cartilage CS/DS

It is useful to compare the levels of expression of particular CS/DS oligosaccharide structures among cartilage samples from different origin. This example compares non-reducing end, internal and linker region oligosaccharides for four separate juvenile bovine samples from two different donors: JB-A1, JB-B1, JB-B2, JB-B3; and five adult human cartilage samples from five different donors: H-A2, H-B1, H-C1, H-D1, and H-E1. The human samples were obtained from discarded surgical samples from patients undergoing total knee replacement. For these analyses, CS/DS samples were extracted from cartilage using an MS-compatible method [31]. GAGs from cartilage (5-μg) were partially digested with lyase enzymes and reductively aminated using d_4-2AA. An aliquot of partially digested CSA (1-μg) labeled with d_0-2AA was added to each sample as an internal standard. Each d_4-2AA labeled sample was mixed with d_0-internal standard and analyzed using amide-HILIC LC/MS, and the results are shown in Figure 1. As shown in the base peak chromatogram (A), CS/DS oligosaccharides elute in order of increasing size and polarity. As would be expected, the most abundant peaks correspond to Δ-unsaturated structures deriving from the long internal regions of the intact chains.

Previous research shows that using SEC, the Δ (1,1,1) to Δ(4,4,4) oligosaccharides elute over a 10 minute time range. The Δ(4,4,4) and Δ (3,3,3) are not resolved, and Δ(3,3,3) and Δ(2,2,2) are partially resolved [39]. Amide–HILIC chromatography separates Δ(1,1,1) to Δ(6,6,6) oligosaccharides over a time range of 35 minutes, as shown in Figure 1A. All oligosaccharides are baseline resolved. Compositions present in low abundances, including (1,2,2), Δ(2,2,1), (2,3,3), and Δ(3,3,2) are also resolved. This improved chromatographic resolution maximizes the extent to which oligosaccharides of similar size, such as linker tetrasaccharides and Δ(2,2,2) are resolved and facilitates their mass spectrometric detection.

Internal Δ-unsaturated oligosaccharides make up the majority of GAG compositions produced from 30% lyase digestion from juvenile bovine and adult human connective tissues. Compositions Δ(1,1,1), Δ(2,2,2), Δ(3,3,3), and Δ(4,4,4) summed to an average 66.2% of the total ion abundance (TIA) in juvenile bovine cartilage and 54.0% of the TIA in adult human cartilage. As shown in Figure 2, the Δ(2,2,2) is the major contributor; averaging 49.1% for

juvenile bovine and 36.9% for adult human. The remaining portion of the sample consists of lower abundance oligosaccharide compositions. These compositions include non-reducing end saturated structures of varying chain length, linker region structures and over-/under-sulfated Δ-unsaturated oligosaccharide structures. The eighteen different cartilage oligosaccharide compositions detected by amide-HILIC LC/MS are displayed in Scheme I. The three most abundant ions corresponding to the saturated non-reducing end are (1,2,2), (2,2,2) and (3,3,3) oligosaccharide chains, adding up collectively on average to 16.0% TIA for juvenile bovine cartilage samples and 24.2% for adult human cartilage samples (Figure 2). The ratio of Δ-unsaturated to saturated ion abundances are 3.9 for juvenile bovine and 2.2 for adult human cartilage. Saturated structures are not detected for oligosaccharides larger than (3,3,3). Adult human cartilage has a lower percentage of Δ-unsaturated oligosaccharides and therefore exhibits shorter chain lengths than juvenile bovine cartilage. The cellularity of each individual tissue varies and it is useful to view the MS ion abundances normalized to the quantity of DNA present in the tissue. The normalized MS ion abundances of the oligosaccharide structures detected in healthy juvenile bovine cartilage and diseased adult human cartilage are shown in Figure 1 of the supplemental data section.

The percent TIA results show that the non-reducing chain population terminates in both HexA and GalNAc, and are consistent with previous literature reports [25]. The percent of juvenile bovine cartilage chains terminating with oligosaccharides with non-reducing terminal HexA, range from 49.0% ± 0.9 to 80.2% ± 1.1. Those from adult human cartilage chains range from 69.6% ± 4.9 to 87.2% ± 0.3. A complete list of the results from determinations of MS percent total ion abundance are listed as ratios in Table 1.

Abundances of Δ-unsaturated oligosaccharide ions correspond to the internal region of the parent CS/DS chains. Values for Δ-unsaturated under-sulfated compositions in which there are fewer sulfate groups than GalNAc residues are on average higher for juvenile bovine cartilage (Figure 2). For juvenile bovine cartilage, the percent of under-sulfated compositions (Δ(2,2,1) and Δ(3,3,2)) range from 7.5% ± 0.5 to 17.2% ± 0.5. The same Δ-unsaturated under-sulfated structures in adult human cartilage are less abundant and range from 4.0% ± 0.1 to 9.6% ± 0.2.

The percentage of linker oligosaccharides that are modified with sulfate and/or phosphate is higher in adult human cartilage. Taken as a percentage of all linker oligosaccharides ions, juvenile bovine cartilage is predominantly unmodified. On average, 51.7% of adult human cartilage chains have linker oligosaccharides with one or more sulfate/phosphate groups. Percent ion abundances were calculated for all saturated, Δ-unsaturated and linker region oligosaccharides in both juvenile bovine and adult human cartilage, and the results are displayed in Table 1. It was not possible to acquire tandem mass spectra on the linker oligosaccharides due to their low ion abundances. The positions of sulfate substitution are therefore not known. The sulfate positions shown for linker oligosaccharides in Scheme I are those that are probable based on published results [12–14].

Tandem MS glycoform quantification of juvenile bovine cartilage CS/DS oligosaccharides

Prior to mass spectrometric analysis, 5-μg of d_4-2AA derivatized cartilage oligosaccharides were mixed with 1.0-μg of d_0-2AA derivatized CSA oligosaccharides, termed the reference standard. Oligosaccharides consisted of a mixture of CSA-like (4GlcAβ1-3GalNAc4Sβ1-), CSB-like (4IdoAα1-3GalNac4Sβ1-) and CSC-like (4GlcAβ1-3GalNAc6Sβ1-) glycoforms. Derivatized d_4-2AA-oligosaccharides (3-μg and 1-μg) were mixed with 0.5-μg and 0.3-μg of d_0-2AA derivatized CSA oligosaccharides, respectively. Due to the increased sensitivity of the amide–HILIC-LC/MS (detection limits 1 μg GAG), in comparison to SEC-LC/MS (detection limits 10 μg GAG) [39], it was possible to acquire tandem mass spectra for 2-AA labeled Δ(2,2,2), Δ(3,3,3), and Δ(4,4,4) extracted from juvenile bovine cartilage samples. The mixture composition of each oligosaccharide chain was determined from the abundances of three

diagnostic product ions; Y_1^{1-}, Y_3^{2-}, and $[M\text{-}H\text{-}SO_3]^{2-}$, respectively for Δ (2,2,2) [39], and Y_3^{2-}, Y_5^{3-}, and $[M\text{-}H\text{-}SO_3]^{3-}$, respectively for Δ(3,3,3) and Y_3^{2-}, Y_5^{3-}, and $[M\text{-}H\text{-}SO_3]^{4-}$, respectively for Δ(4,4,4). The percent total ion abundances of the heavy forms of the diagnostic ions were calculated and inserted into a system of three equations and three unknowns [47–49] using coefficients calculated from the ion abundances for the same diagnostic ions from purified CSA, CSB and CSC standards.

The percentages of the isomeric glycoforms of CSA, CSB and CSC in Δ(2,2,2) extracted from, for example, 5-μg intact juvenile bovine cartilage donor B explant 3, shown in Figure 2 of the supplemental data section, were calculated as the mean values from 3 separate aliquots and were found to be 40.8% ± 2.7, 1.4% ± 0.3, and 57.8% ± 2.6, respectively. The glycoform percentage for Δ(3,3,3) was found to be 42.0% ± 1.1, 1.0% ± 0.3, and 57.0% ± 0.8, respectively; and 43.8% ± 1.7, 0.9% ± 0.8, and 55.3% ± 2.1, respectively, for Δ(4,4,4) from the same 5-μg juvenile bovine donor B explant 3 sample (representative data shown in Table 2). The total experimental error for measurement of each glycoform was low and within the range previously reported for Δ(2,2,2) from this sample set using SEC-LC/MS/MS [31].

Given the non-specific nature of the chondroitinase enzymes used, the glycoforms of each chain length are likely to reflect the overall CS chain composition. The comparison of Δ(2,2,2), Δ(3,3,3), and Δ(4,4,4) glycoform percentages illustrates this fact. Extracted CS GAGs from three additional intact bovine cartilage tissues, labeled juvenile bovine A-1, B-1 and B-2 were analyzed. The results demonstrate that the amide-HILIC method is scaleable, allowing for quantification of low microgram amounts of material. The complete results of 1-μg, 3-μg, and 5-μg quantities of quantified Δ(2,2,2), Δ(3,3,3), and Δ(4,4,4) internal oligosaccharides for all juvenile bovine cartilage samples are listed in Table 1 of the supplemental data section.

Quantification of adult human cartilage

Papain digests of adult human knee cartilage were divided into aliquots of 1-μg, 3-μg, and 5-μg GAG-equivalent using DMMB assay results. Triplicate aliquots were extracted, purified and analyzed by amide-HILIC-ESI-LC/MS/MS with a d_0-2AA-CSA internal standard, in the same manner as that of the juvenile bovine cartilage. Glycoform percentages of CSA, CSB, and CSC from LC-tandem mass spectra results of Δ(2,2,2), Δ(3,3,3), and Δ(4,4,4) internal oligosaccharide chains from, for example, adult human cartilage (5-μg) donor B explant 1 were found to be 4.5% ± 1.2, 0.7% ± 0.1, and 94.9% ± 1.1, respectively for Δ(2,2,2). Δ(3,3,3) GAG chains were found to be 5.9% ± 0.4, 0.3% ± 0.1, and 93.8% ± 0.4, respectively; and 7.1% ± 2.2, 2.3% ± 1.8, and 90.6% ± 1.6, respectively, for Δ(4,4,4). Representative results are shown in Table 2. A series of adult human cartilage explants (5 explants from 5 separate donors) was used to demonstrate the optimization and increased sensitivity of this analytical platform for human samples. The percentages of the isomeric glycoforms of CSA, CSB and CSC determined for each different size oligosaccharide chain from intact adult human cartilage samples are listed in Table 2 of the supplemental data section.

Product ion analysis of structurally significant cartilage CS/DS oligosaccharides

The product ion abundances of Δ(2,2,2) are compared between juvenile bovine and adult human cartilage in Figure 3A. Product ions include glycosidic bond cleavages of B-, C-, and Y-types; cross-ring cleavage X, and loss of sulfate ions [50]. The percent TIA of each product ion varies between normal (juvenile bovine) and osteoarthritic (adult human) cartilage samples. Visual inspection shows several ions differing in abundance, indicating glycoform differences between the two samples. Using pair – wise statistical comparisons, it can be concluded that a significant ion abundance difference exists between tissue samples for product ions $[Y_1\text{-}SO_3]$, Y_1, $^{0,2}X_1$, B_3, and $[Y_3\text{-}2SO_3]$.

Figure 3B compares product ion abundances for Δ(3,3,3) among the cartilage tissue samples. Pairwise statistical comparisons conclude that the Y_1^{1-} and the Y_2^{1-} product ions have statistically significant differences in ion abundance between normal and diseased cartilage samples. Figure 3C compares product ion abundances produced in the tandem mass spectra of Δ(4,4,4). Using pair-wise comparisons, the $[M\text{-}4H\text{-}SO_3]^{4-}$ and Y_3^{2-} product ions were calculated to have a statistically significant difference between normal and diseased cartilage samples. These data illustrate the principle of glycoform comparison of GAG glycoform expression.

Amide-HILIC MS of joint tissues

On-line capillary amide-HILIC LC/MS results for juvenile bovine muscle, ligament, tendon and synovium connective joint tissues are shown in Figure 4. Abundances of internal oligosaccharides Δ(1,1,1), Δ(2,2,2) and Δ(3,3,3) correspond to 55.4% of the total ion abundance (TIA) in muscle, as shown in Figure 4, 70.2% of the TIA in ligament, 77.0% in tendon, and 57.0% of the TIA in synovium. The abundances of saturated structures deriving from the non-reducing chain termini, (1,2,2), (2,2,2), (2,3,3) and (3,3,3) correspond to 24.9% TIA in muscle, and 13.8%, 14.5% and 27.1% of the TIA in ligament, tendon and synovium, respectively. The ratio of Δ-unsaturated to saturated ion abundances are 2.6 ± 0.1 for muscle, 2.4 ± 0.2 for synovium and 5.6 ± 0.3 for ligament and tendon (See Table 1 for complete list). Muscle and synovium have a lower percentage of Δ-unsaturated oligosaccharides and therefore exhibit shorter chain lengths than both tendon and ligament. In all four connective tissues, the ion corresponding to Δ(2,2,2) is highest in abundance; averaging 42.4% of the total. The MS ion abundances of all oligosaccharide structures, both low and high abundance, normalized to quantity of DNA in each connective tissue sample are shown in the supplemental data section in Figure 3. Juvenile bovine cartilage donor B3 has been added to the graph as a point of reference to compare the cartilage and connective tissue samples. Cartilage displays normalized MS ion abundances approximately two times greater than those of the other connective tissues, consistent with lower cellularity.

Among the connective tissues, the percent of chains with non-reducing end terminal HexA range from 69.9% ± 1.1 (ligament) to 88.8% ± 1.0 (muscle). Muscle and synovium exhibit the shortest CS/DS chain lengths, and the abundances of GAGs relative to DNA are lowest for these tissues. Linker region oligosaccharide compositions are significantly lower in abundances in comparison to the same compositions for the cartilage samples. The percent of linker region oligosaccharides with one or more sulfate/phosphate groups is 31.2% ± 3.1 in tendon, 40.9% ± 0.8 in ligament, and 67.0% ± 3.1 in muscle. Linker oligosaccharides were not detected in synovium tissue. A complete list of results is detailed in Table 1.

Quantification of other connective tissue samples

Juvenile bovine muscle, ligament, tendon and synovium samples (5-μg GAG-equivalent) were extracted and purified using the streamlined multi-step GAG extraction protocol described [31], and analyzed using the capillary amide-HILIC-ESI-LC-MS/MS method. The same diagnostic fragment ions used for quantification of Δ(2,2,2), Δ(3,3,3) and Δ(4,4,4) cartilage samples were used for the quantification of the various connective tissues. For example, in ligament, the glycoform percentage of CSA, CSB, and CSC for Δ(2,2,2) was found to be 2.3% ± 1.1, 43.2% ± 1.6, and 54.5% ± 0.4, respectively. Δ(3,3,3) GAG chains were found to be 2.3% ± 0.2, 42.4% ± 0.3, and 55.3% ± 0.3, respectively; and 2.7% ± 0.4, 44.2% ± 0.9, and 53.1% ± 0.5, respectively, for Δ(4,4,4). A complete list of quantification results for juvenile bovine connective tissues are given in Table 2. Juvenile bovine muscle lacked an abundant enough Δ(4,4,4) tandem signal for quantification.

While adult human cartilage tissue displays a high level of CSC-like (4GlcAβ1-3GalNAc6Sβ1-) repeats, juvenile bovine cartilage shows a mixture of CSA-like (4GlcAβ1-3GalNAc4Sβ1-) (46.2%) and CSC-like repeats. There is little or no CSB-like (DS) (4IdoAα1-3GalNAc4Sβ1-) content of cartilage, reflecting the fact that levels of the glucuronyl C5-epimerase is low in this tissue [51]. Further diversity is found among synovium, ligament, muscle and tendon. The characteristics of the oligosaccharides are also indicative of specific cores and in this case a high content of CSB like repeats would be indicative of decorin. The CS/DS glycoforms of decorin are tissue dependent [31,39,52]. These analyses provide an excellent rationale for analyzing GAG phenotypes among different tissues.

4. Discussion

Relative to previous work, the amide-HILIC chromatography platform allowed a ten-fold decrease in sample size, to as low as 1-μg GAG-equivalent tissue samples. The goal was, not only to decrease the starting sample quantity, but to also generate increased detail in profiling structural changes to connective tissue-derived GAGs during developmental and disease processes. Previously, it was found possible to detail glycoform abundance changes in only internal tetrasaccharide GAG chains. However, the amide-HILIC LC-MS/MS platform enabled quantification of internal tetrasaccharide, hexasaccharide, and octasaccharide GAG chains, as well as non-reducing end saturated and linker region oligosaccharides from both juvenile bovine and adult human cartilage and connective tissue samples. Amide-HILIC LC/MS analysis provided both the sensitivity and resolution needed to detect eighteen different oligosaccharide compositions in the cartilage samples (Scheme I). The eighteen compositions were made up of nine internal oligosaccharide chains, including three under-/over-sulfated chains, four non-reducing end saturated structures, and five reducing end linker region structures. The compositions detected ranged in abundances, with the highest (Δ(2,2,2)) averaging approximately 49% TIA, and the lowest (Δ(2,2,3)) being on average approximately 1.0% TIA. Differences in LC/MS percent total ion abundances between the healthy and diseased cartilage tissues, given in detail in the results section, demonstrate that the three domains that make up a GAG chain change during disease development and maturation. The results are complementary to those obtained using graphitized carbon LC/MS on aggrecan CS chains [14]. Graphitized carbon chromatographically resolves 4- and 6-sulfated disaccharides as well as linker tetrasaccharides obtained from exhaustive chondroitinase digestion. The amide-HILIC LC/MS approach in the present work enable analysis of extended CS oligosaccharides.

Several age-related increases in the ratio of 6- to 4-sulfated GalNAc residues in articular cartilage CS have been reported [5,23,27,30,53]. In adult articular cartilage CS 6-sulfation is known to dominate over non-sulfated and 4-sulfated GalNAc residues [5]. The MS results presented herein on 1-μg, 3-μg and 5-μg GAG-equivalent tissue samples from different explant locations of cartilage in different species agree with the previous findings for the age-related compositions of GAGs in cartilage tissues. Therefore, a decrease in sample quantity does not jeopardize the content or quality of information that can be acquired from a GAG chain extracted from an intact tissue sample.

Given the non-specific nature of the chondroitinase enzymes used, the glycoform percentage of a Δ(2,2,2) GAG chain should hypothetically reflect the overall CS chain composition. Oligosaccharide analysis of Δ(2,2,2), Δ(3,3,3) and Δ(4,4,4) from the same juvenile bovine and adult human cartilage samples resulted in significantly similar signature ion profiles and quantification values (supplemental data Tables 1 and 2). With glycoform percentages all within approximately 1–2% of one another, it is shown here that GAG chains of varying size can be quantified to reflect the overall CS chain composition in the tissue sample.

To demonstrate the applicability of the amide-HILIC LC-MS/MS platform to tissues other than cartilage, detailed MS and tandem MS structural characterization was completed on four healthy juvenile bovine connective tissues. Intact juvenile bovine muscle, tendon, ligament and synovium tissues were shown to be compatible with the streamlined multi-step cartilage GAG extraction protocol [31], and required no additional purification steps such as delipidation or defatting. LC/MS data shows that the amide-HILIC platform is able to detect all eighteen compositions (Scheme I) in each of the four connective tissue samples. The MS percent total ion abundances of the different oligosaccharide compositions vary between the different tissues, as shown in Figure 4. Future experiments can therefore be focused around the structural characterization of several connective tissues at various stages in a disease process, such as osteoarthritis. Tandem MS results on the glycoform quantification of connective tissues showed high levels of DS glycoforms, in muscle, tendon and ligament, a result which is consistent with previous literature reports [35–38]. The CSB content ranged from approximately 43% in juvenile bovine tendon and ligament to approximately 59% in juvenile bovine muscle (Table 2). The GAG chains in tendon and ligament have previously been shown to undergo changes in composition during maturation [34], therefore future experiments may be focused on glycoform quantification of aged or diseased connective tissues, in the same manner that cartilage was analyzed in this study.

The analysis presented herein enables simultaneous profiling of the expression of non-reducing end, linker region, and Δ-unsaturated interior oligosaccharide domains of CS chains among five different joint tissues. The procedure employs a sensitive amide-HILIC LC-MS/MS platform that is applicable to microgram quantities of proteoglycans from various joint tissues. The results provide important new information on the changes to the expression of CS GAG chains, which may lead to novel GAG structural characterizations during disease and development.

Supplementary Material

Refer to Web version on PubMed Central for supplementary material.

Acknowledgements

We thank Drs. Thomas Thornhill and John Wright for providing discarded tissues. Funding from NIH grants P41 RR10888 and R01 HL74197 is gratefully acknowledged. Bruker Daltonics donated the Esquire 3000 ion trap mass spectrometer used in this work.

Abbreviations

CS
: chondroitin sulfate

CSA
: chondroitin sulfate type A

CSB
: chondroitin sulfate type B

CSC
: chondroitin sulfate type C

DMMB
: dimethylmethylene blue

dp

degree of polymerization

DS
dermatan sulfate

GAG
glycosaminoglycan

HILIC
hydrophilic interaction chromatography

HS
heparan sulfate

LC-MS/MS
liquid chromatography-tandem mass spectrometry

OA
osteoarthritis

PG
proteoglycan

SLRP
small leucine-rich proteoglycan

2-AA
2-anthranilic acid

Δ-unsaturation
delta-unsaturation

Δ(1,1,1)
delta unsaturated disaccharide

Δ(2,2,2)
delta unsaturated tetrasaccharide

Δ(3,3,3)
delta unsaturated hexasaccharide

Δ(4,4,4)
delta unsaturated octasaccharides

References

1. Silbert JE, Sugumaran G. Biosynthesis of chondroitin/dermatan sulfate. IUBMB Life 2002;54:177–186. [PubMed: 12512856]
2. Fransson LA, Belting M, Jonsson M, Mani K, et al. Biosynthesis of decorin and glypican. Matrix Biol 2000;19:367–376. [PubMed: 10963998]
3. Seidler DG, Breuer E, Grande-Allen KJ, Hascall VC, Kresse H. Core protein dependence of epimerization of glucuronosyl residues in galactosaminoglycans. J Biol Chem 2002;277:42409–42416. [PubMed: 12207034]
4. Bulow HE, Hobert O. The Molecular Diversity of Glycosaminoglycans Shapes Animal Development. Annu Rev Cell Dev Biol 2006;22:375–407. [PubMed: 16805665]
5. Bayliss MT, Osborne D, Woodhouse S, Davidson C. Sulfation of chondroitin sulfate in human articular cartilage. The effect of age, topographical position, and zone of cartilage on tissue composition. J Biol Chem 1999;274:15892–15900. [PubMed: 10336494]

6. Maroudas AI. Balance between swelling pressure and collagen tension in normal and degenerate cartilage. Nature 1976;260:808–809. [PubMed: 1264261]
7. Hassell JR, Kimura JH, Hascall VC. Proteoglycan core protein families. Annu Rev Biochem 1986;55:539–567. [PubMed: 3527051]
8. Malmstrom A, Fransson LA. Biosynthesis of dermatan sulfate. I. Formation of L-iduronic acid residues. J Biol Chem 1975;250:3419–3425. [PubMed: 1123348]
9. Kitagawa H, Oyama M, Masayama K, Yamaguchi Y, Sugahara K. Structural Variations in the glycosaminoglycan-protien linkage region of recombinant decorin expressed in Chinese hamster ovary cells. Glycobiology 1997;7:1175–1180. [PubMed: 9455918]
10. Sugahara K, Mikami T, Uyama T, Mizuguchi S, Nomura K, Kitagawa H. Recent Advances in the Structural Biology of Chondroitin Sulfate and Dermatan Sulfate. Curr Opin Struct Biol 2003;13:612–620. [PubMed: 14568617]
11. Sugahara K, Yamashina I, De Waard P, Van Halbeek H, Vliegenthart JF. Structural studies on sulfated glycopeptides from the carbohydrate-protein linkage region of chondroitin 4-sulfate proteoglycans of swarm rat chondrosarcoma. Demonstration of the structure Gal(4-O-sulfate)beta 1-3Gal beta 1-4XYL beta 1-O-Ser. J Biol Chem 1988;263:10168–10174. [PubMed: 3134345]
12. Cheng F, Heinegard D, Fransson L, Bayliss M, et al. Variations in the chondroitin sulfate-protein linkage region of aggrecans from bovine nasal and human articular cartilages. J Biol Chem 1996;271:28572–28580. [PubMed: 8910487]
13. de Beer T, Inui A, Tsuda H, Sugahara K, Vliegenthart JF. Polydispersity in sulfation profile of oligosaccharide alditols isolated from the protein-linkage region and the repeating disaccharide region of chondroitin 4-sulfate of bovine nasal septal cartilage. Eur J Biochem 1996;240:789–797. [PubMed: 8856085]
14. Estrella RP, Whitelock JM, Packer NH, Karlsson NG. Graphitized carbon LC-MS characterization of the chondroitin sulfate oligosaccharides of aggrecan. Anal Chem 2007;79:3597–3606. [PubMed: 17411012]
15. Sakaguchi H, Watanabe M, Ueoka C, Sugiyama E, et al. Isolation of reducing oligosaccharide chains from the chondroitin/dermatan sulfate-protein linkage region and preparation of analytical probes by fluorescent labeling with 2-aminobenzamide. J Biochem (Tokyo) 2001;129:107–118. [PubMed: 11134964]
16. Sugahara K, Ohkita Y, Shibata Y, Yoshida K, Ikegami A. Structural Studies on the Hexasaccharide Alditols Isolated from the Carbohydrate-Protein Linkage Region of Dermatan Sulfate Proteoglycans of Bovine Aorta. J Biol Chem 1995;270:7204–7212. [PubMed: 7706259]
17. Hynds DL, Snow DM. Neurite Outgrowth inhibition by chondroitin sulfate proteoglycan: stalling/stopping exceeds turning in human neuroblastoma growth cones. Experimental Neurology 1999;160:244–255. [PubMed: 10630209]
18. Gilbert RJ, McKeon RJ, Darr A, Calabro A, et al. CS-4,6 is differentially upregulated in glial scar and is a potent inhibitor of neurite extension. Molecular And Cellular Neuroscience 2005;29:545–558. [PubMed: 15936953]
19. Chai W, Beeson JG, Lawson AM. The structural motif in chondroitin sulfate for adhesion of Plasmodium falciparum-infected erythrocytes comprises disaccharide units of 4-*O*-sulfated and non-sulfated *N*-acetylgalactosamine linked to glucuronic acid. J Biol Chem 2002;277:22438–22446. [PubMed: 11956186]
20. Trowbridge JM, Gallo RL. Dermatan sulfate: new functions from an old glycosaminoglycan. Glycobiology 2002;12:117R–125R.
21. Menozzi FD, Pethe K, Bifani P, Soncin F, Brennan MJ, Locht C. Enhanced bacterial virulence through exploitation of host glycosaminoglycans. Mol Microbiol 2002;43:1379–1386. [PubMed: 11971262]
22. Mardberg K, Trybala E, Tufaro F, Bergstrom T. Herpes simplex virus type 1 glycoprotein C is necessary for effecient infection of chondroitin sulfate-expressing gro2C cells. J Gen Virol 2002;83:291–300. [PubMed: 11807221]
23. Belcher C, Yaqub R, Fawthrop F, Bayliss M, Doherty M. Synovial fluid chondroitin and keratan sulphate epitopes, glycosaminoglycans, and hyaluronan in arthritic and normal knees. Ann Rheum Dis 1997;56:299–307. [PubMed: 9175930]

24. Hazell PK, Dent C, Fairclough JA, Bayliss MT, Hardingham TE. Changes in glycosaminoglycan epitope levels in knee joint fluid following injury. Arthritis Rheum 1995;38:953–959. [PubMed: 7541993]
25. Plaas AH, West LA, Wong-Palms S, Nelson FR. Glycosaminoglycan sulfation in human osteoarthritis. Disease-related alterations at the non-reducing termini of chondroitin and dermatan sulfate. J Biol Chem 1998;273:12642–12649. [PubMed: 9575226]
26. Shinmei M, Miyauchi S, Machida A, Miyazaki K. Quantitation of chondroitin 4-sulfate and chondroitin 6-sulfate in pathologic joint fluid. Arthritis Rheum 1992;35:1304–1308. [PubMed: 1445446]
27. Kitagawa H, Tsutsumi K, Tone Y, Sugahara K. Developmental Regulation of the Sulfation Profile of Chondroitin Sulfate Chains in the Chicken Embryo Brain. J Biol Chem 1997;272:31377–31381. [PubMed: 9395468]
28. Mark MP, Butler WT, Ruch JV. Transient expression of a chondroitin sulfate-related epitope during cartilage histomorphogenesis in the axial skeleton of fetal rats. Dev Biol 1989;133:475–488. [PubMed: 2471655]
29. Tufvesson E, Malmstrom J, Marko-Varga G, Westergren-Thorsson G. Biglycan isoforms with differences in polysaccharide substitution and core protein in human lung fibroblasts. Eur J Biochem 2002;269:3688–3696. [PubMed: 12153565]
30. Roughley PJ, White RJ. Age-related changes in the structure of the proteoglycan subunits from human articular cartilage. J Biol Chem 1980;255:217–224. [PubMed: 7350154]
31. Hitchcock AM, Yates KE, Shortkroff S, Costello CE, Zaia J. Optimized extraction of glycosaminoglycans from normal and osteoarthritic cartilage for glycomics profiling. Glycobiology 2006;17:25–35. [PubMed: 16980326]
32. Plaas AH, Wong-Palms S, Roughley PJ, Midura RJ, Hascall VC. Chemical and immunological assay of the nonreducing terminal residues of chondroitin sulfate from human aggrecan. J Biol Chem 1997;272:20603–20610. [PubMed: 9252375]
33. West LA, Roughley P, Nelson FR, Plaas AH. Sulphation heterogeneity in the trisaccharide (GalNAcSbeta1, 4GlcAbeta1,3GalNAcS) isolated from the non-reducing terminal of human aggrecan chondroitin sulphate. Biochem J 1999;342:223–229. [PubMed: 10432320]
34. Rees SG, Flannery CR, Little CB, Hughes CE, et al. Catabolism of aggrecan, decorin and biglycan in tendon. Biochem J 2000;350:181–188. [PubMed: 10926842]
35. Watanabe M, Nojima M, Shibata T, Hamada M. Maturation-related biochemical changes in swine anterior cruciate ligament and tibialis posterior tendon. J Orthop Res 1994;12:672–682. [PubMed: 7931784]
36. Watanabe K, Oohira A, Uramoto I, Totsuka T. Age-Related Changes in the Content and Composition of Glycosaminoglycans Isolated from the Mouse Skeletal Muscle: Normal and Dystrophic Conditions. J Biochem 1986;100:167–173. [PubMed: 3759927]
37. Toledo OM, Dietrich CP. Tissue specific distribution of sulfated mucopolysaccharides in mammals. Biochim Biophys Acta 1977;498:144–122.
38. Nakano T, Sunwoo HH, Li XJ, Price MA, Sim JS. Study of sulfated glycosaminoglycans from porcine skeletal muscle epimysium including analysis of iduronosyl and glucuronosyl residues in galactosaminoglycan fractions. J Agric Food Chem 1996;44:1424–1434.
39. Hitchcock AM, Costello CE, Zaia J. Glycoform quantification of chondroitin/dermatan sulfate using an LC/MS/MS platform. Biochemistry 2006;45:2350–2361. [PubMed: 16475824]
40. Bigge JC, Patel TP, Bruce JA, Goulding PN, et al. Nonselective and efficient fluorescent labeling of glycans using 2-amino benzamide and anthranilic acid. Anal Biochem 1995;230:229–238. [PubMed: 7503412]
41. Wuhrer M, Koeleman CA, Deelder AM, Hokke CH. Normal-phase nanoscale liquid chromatography-mass spectrometry of underivatized oligosaccharides at low-femtomole sensitivity. Anal Chem 2004;76:833–838. [PubMed: 14750882]
42. Akiyama H, Shidawara S, Mada A, Toyoda H, Toida T, Imanari T. J Chromatogr-Biomed 1992;579:203–207.

43. Saitoh H, Takagaki K, Majima M, Nakamura T, et al. Enzymic reconstruction of glycosaminoglycan oligosaccharide chains using the transglycosylation reaction of bovine testicular hyaluronidase. J Biol Chem 1995;270:3741–3747. [PubMed: 7876114]
44. Guile GR, Rudd PM, Wing DR, Prime SB, Dwek RA. A Rapid High-Resolution High-Performance Liquid Chromatographic Method for Separating Glycan Mixtures and Analyzing Oligosaccharide Profiles. Anal Biochem 1996;240:210–226. [PubMed: 8811911]
45. Mattu TS, Royle L, Langridge J, Wormald MR, Van den Steen PE, Van Damme J, Opdenakker G, Harvey DJ, Dwek RA, Rudd PM. O-Glycan Analysis of Natural Human Neutrophil Gelatinase B Using a Combination of Normal Phase- HPLC and Online Tandem Mass Spectrometry: Implications for the Domain Organization of the Enzyme. Biochemistry 2000;39:15695–15704. [PubMed: 11123894]
46. Wuhrer M, Koeleman CA, Hokke CH, Deelder AM. Protein Glycosylation Analyzed by Normal-Phase Nano-Liquid Chromatography-Mass Spectrometry of Glycopeptides. Anal Chem 2005;77:886–894. [PubMed: 15679358]
47. Desaire H, Leary J. Detection and quantification of the sulfated disaccharides in chondroitin sulfate by electrospray tandem mass spectrometry. J Am Soc Mass Spectrom 2000;11:916–920. [PubMed: 11014453]
48. Desaire H, Leary JA. Utilization of MS^3 spectra for the multicomponent quantification of diastereomeric *N*-acetylhexosamines. J Am Soc Mass Spectrom 2000;11:1086–1094. [PubMed: 11118116]
49. Saad OM, Leary JA. Compositional analysis and quantification of heparin and heparan sulfate by electrospray ionization ion trap mass spectrometry. Anal Chem 2003;75:2985–2995. [PubMed: 12964742]
50. Domon B, Costello CE. A systematic nomenclature for carbohydrate fragmentations in FAB-MS/MS spectra of glycoconjugates. Glycoconjugate J 1988;5:397–409.
51. Tiedemann K, Larsson T, Heinegard D, Malmstrom A. The glucuronyl C5-epimerase activity is the limiting factor in the dermatan sulfate biosynthesis. Arch Biochem Biophys 2001;391:65–71. [PubMed: 11414686]
52. Miller MJC, Costello CE, Malmström A, Zaia J. A tandem mass spectrometric approach to determination of chondroitin/dermatan sulfate oligosaccharide glycoforms. Glycobiology 2006;16:502–513. [PubMed: 16489125]
53. Lauder RM, Huckerby TN, Brown GM, Bayliss MT, Nieduszynski IA. Age-related changes in the sulphation of the chondroitin Sulphate linkage region from human articular cartilage aggrecan. Biochem J 2001;358:523–528. [PubMed: 11513754]

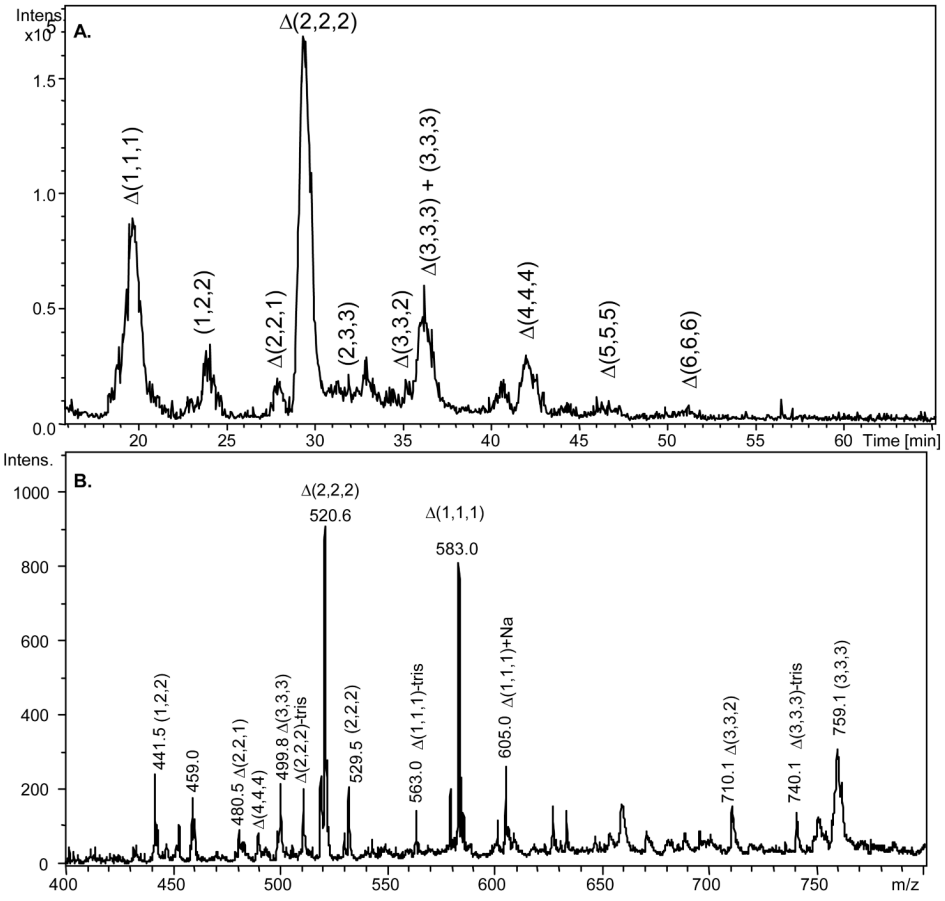

Figure 1.

A. Base peak chromatogram (100–800 *m/z*) of 30% chondroitin lyase depolymerized CS/DS from 5-μg d_4-2AA-juvenile bovine cartilage mixed with 1-μg d_0-2AA-CSA internal oligosaccharide standard. GAG oligosaccharide chains ranging from disaccharide to dodecasaccharide elute from 15 to 55 minutes. Oligosaccharide compositions are given as (HexA, GalNAc, SO_3) (X,Y,Z), with 4,5-unsaturation shown as Δ. B. The average mass spectrum of all eluted oligosaccharides in the sample mixture. Label of tris indicates reductive amination product with tris buffer.

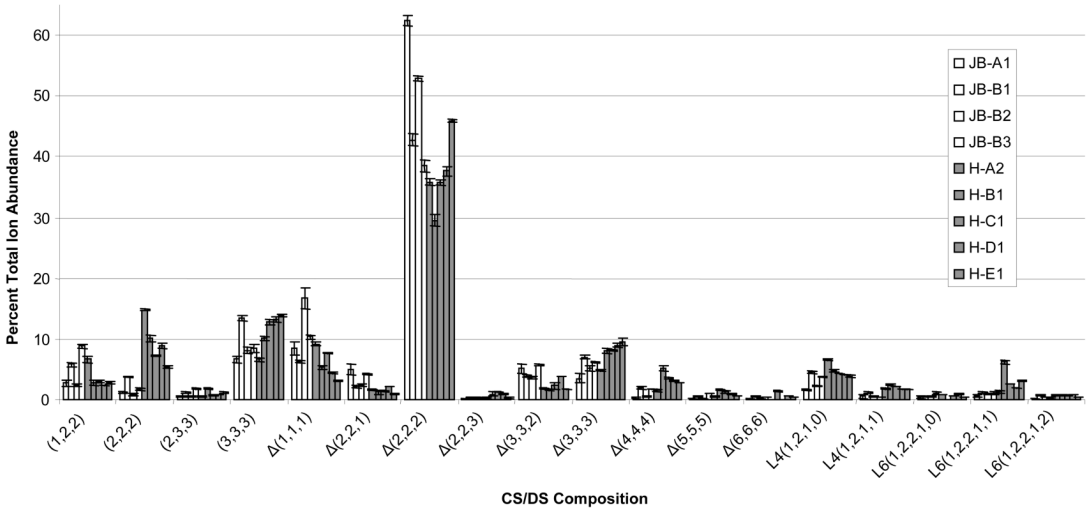

Figure 2.

MS percent total ion abundances of all oligosaccharide chains present in all juvenile bovine and adult human cartilage samples. Oligosaccharide compositions are given as (HexA, GalNAc, SO_3) (X,Y,Z), with Δ indicating 4,5-unsaturation of the non-reducing terminal HexA residue. Tetrasaccharide linker compositions are given as (Xyl, Gal, HexA, SO_3) (V,W,X,Z). Hexasaccharide linker compositions are given as (Xyl, Gal, HexA, GalNAc, SO_3) (V,W,X,Y,Z).

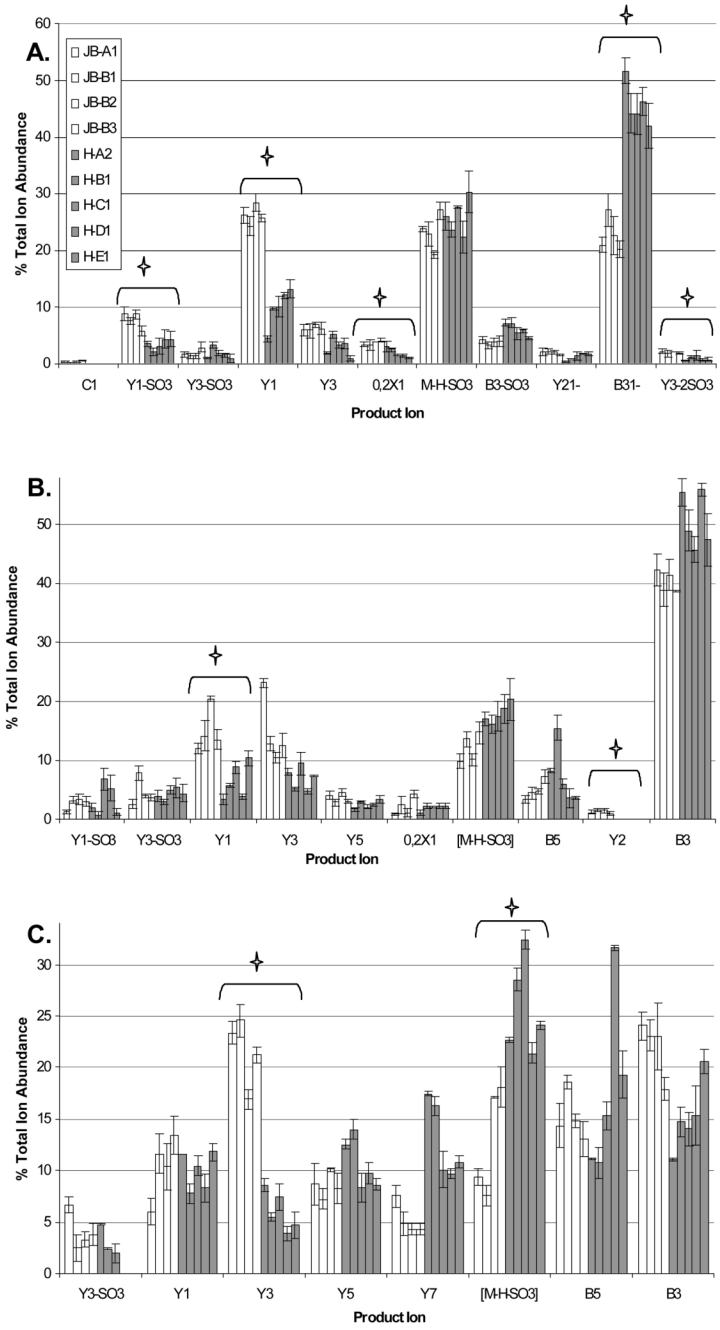

Figure 3.

A. The percent total ion abundance of all product ions produced in the tandem mass spectra of Δ(2,2,2) B. The percent total ion abundance of all product ions produced in the tandem mass spectra of Δ(3,3,3) C. The percent total ion abundance of all product ions produced in the tandem mass spectra of Δ(4,4,4). X, Y and [M-H-$S0_3$] ions correspond to cartilage product ions containing the reducing end and therefore the d_4-2-anthranilic acid tag. B and C ions correspond to the non-reducing end, which does not contain the stable isotope tag, and therefore contain a mixture of cartilage and internal standard. The star denotes product ions that have a statistical difference in ion abundance between the healthy and diseased tissues. The key shown in graph A is applicable to each of the three graphs.

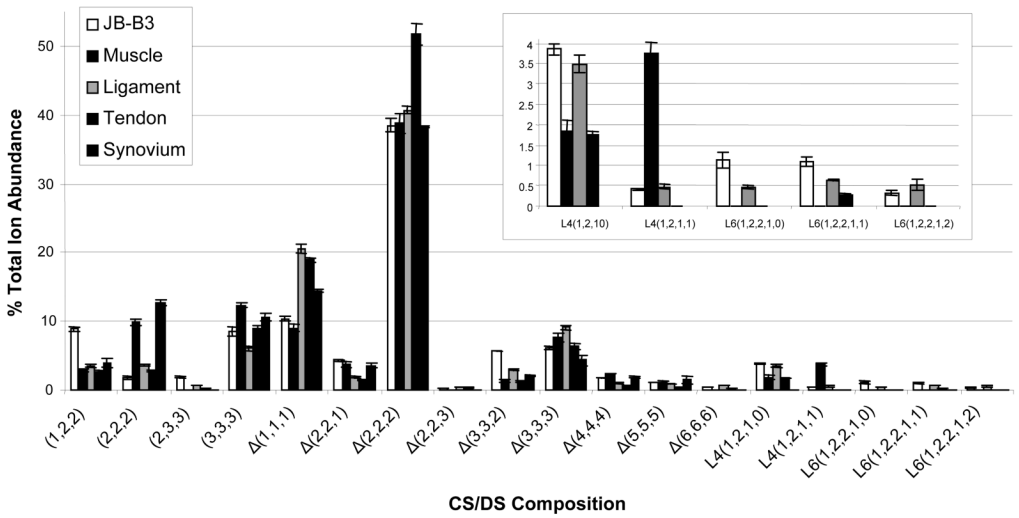

Figure 4.

MS percent total ion abundances of all oligosaccharide chains present in all connective tissue samples from juvenile bovine muscle, ligament, tendon and synovium. Linker region oligosaccharide compositions are expanded in order to see lower abundance structures. Oligosaccharide compositions are given as (HexA, GalNAc, SO_3) (X,Y,Z), with Δindicating 4,5-unsaturation of the non-reducing terminal HexA residue. Tetrasaccharide linker oligosaccharides compositions are given as (Xyl, Gal, HexA, SO_3) (V,W,X,Z). Hexasaccharide linker oligosaccharide compositions are given as (Xyl, Gal, HexA, GalNAc, SO_3) (V,W,X,Y,Z). Cartilage has been added to the connective tissue graphs as a point of reference.

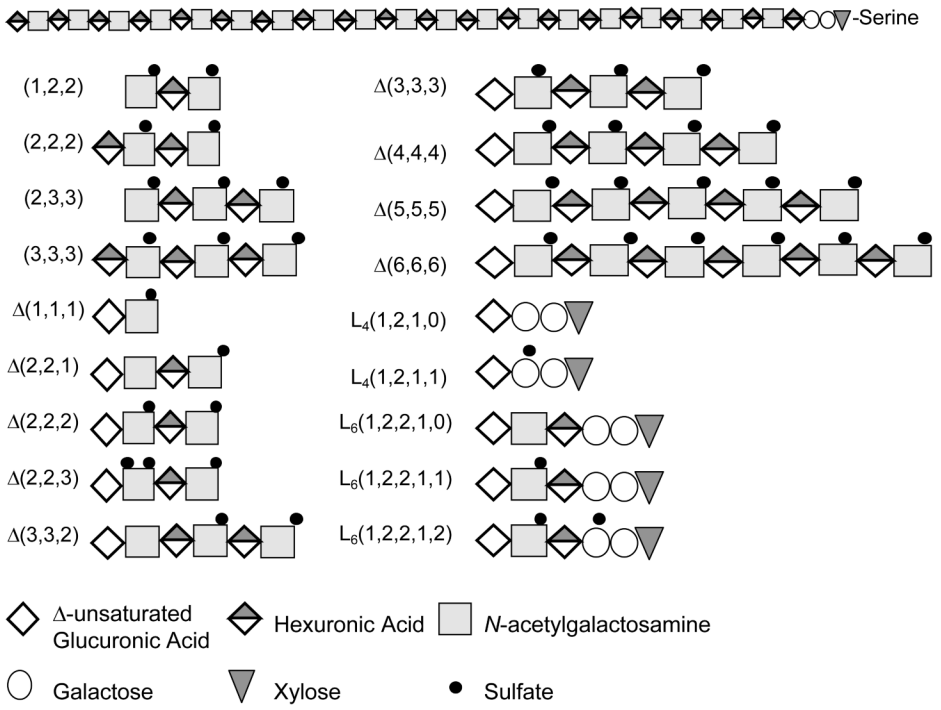

Scheme I.

The oligosaccharide compositions of eighteen different structures found in connective tissue samples by HILIC-amide LC/MS. The compositions include Δ-unsaturated internal oligosaccharides, over-/under-sulfated Δ-unsaturated oligosaccharides, non-reducing end saturated structures of varying chain length and linker region structures. Oligosaccharide compositions are given as (HexA, GalNAc, SO_3) (X,Y,Z), with 4,5-unsaturation shown as Δ. L_4 represents the tetrasaccharide linker and L_6 represents the hexasaccharide linker oligosaccharide. Internal hexuronic acids may be either glucuronic acid or iduronic acid. Sulfates residing on the galactose and *N*-acetylgalactosamine have been arbitrarily placed. Sulfates on the *N*-acetylgalactosamine may be positioned on either the 4- or 6-position. The second sulfate on Δ(2,2,3) may be positioned on either of the two *N*-acetylgalactosamines.

Table 1

Complete list of LC/MS total ion abundance ratios and percentages for all connective tissue samples. Ratios and percentages are shown as the average of triplicate runs of each tissue sample.

Tissue Sample	Δ-unsaturated/saturated	% TIA/μg DNA[a]	% Non- reducing end terminal HexA[b]	% Under- sulfated Δ-unsaturated[c]	% unsulfated linker[d]
JB-Cartilage A1	7.7 ± 0.6	N/A	75.5 ± 4.0	11.9 ± 0.9	61.0 ± 7.1
JB-Cartilage B1	2.7 ± 0.1	2.8	76.1 ± 1.7	9.1 ± 0.5	61.9 ± 2.8
JB-Cartilage B2	6.9 ± 0.6	2.1	80.2 ± 1.1	7.5 ± 0.5	59.6 ± 1.8
JB-Cartilage B3	2.8 ± 0.1	2.3	48.9 ± 0.9	17.2 ± 0.5	73.3 ± 1.3
H- Cartilage A2	1.9 ± 0.1	13.7	74.9 ± 1.6	6.4 ± 0.4	66.4 ± 2.7
H- Cartilage B1	2.3 ± 0.1	18.5	69.6 ± 4.9	4.7 ± 0.3	33.2 ± 1.2
H- Cartilage C1	2.6 ± 0.1	47.6	83.9 ± 0.8	6.1 ± 0.8	47.9 ± 0.4
H- Cartilage D1	2.5 ± 0.1	28.6	87.2 ± 0.3	9.6 ± 0.2	52.5 ± 0.8
H- Cartilage E1	2.8 ± 0.2	22.2	83.0 ± 1.3	4.0 ± 0.1	45.4 ± 1.4
JB-Muscle	2.6 ± 0.1	2.3	88.8 ± 1.0	7.7 ± 0.7	33.0 ± 3.1
JB-Ligament	5.6 ± 0.3	9.2	69.9 ± 1.1	6.1 ± 0.3	59.1 ± 0.8
JB-Tendon	5.6 ± 0.3	2.9	80.4 ± 1.5	3.2 ± 0.2	68.8 ± 3.1
JB-Synovium	2.4 ± 0.2	4.4	85.5 ± 1.8	8.6 ± 0.7	0.0 ± 0.0

N/A indicates data not available.

[a] The ratio of the MS ion abundance divided by the μg of DNA present per sample.

[b] The percent of compositions terminating in a reducing end hexuronic acid.

[c] The percent of under-sulfated Δ-unsaturated compositions per tissue sample.

[d] The percent of unmodified linker region compositions as compared to all existing linker oligosaccharides.

Table 2

Glycoform analysis of connective tissues. The percent composition of CSA-like (4GlcAβ1-3GalNAc4Sβ1-), CSB-like (4IdoAα1-3GalNAc4Sβ1-), CSC-like (4GlcAβ1-3GalNAc6Sβ1-) isomers for adult human cartilage and juvenile bovine cartilage, ligament, muscle, tendon and synovium samples. CSA, CSB and CSC standards were used to compare the relative amounts characteristic of each biological sample. Δ(2,2,2) represents the glycoform percentage of an internal Δ-unsaturated tetrasaccharide, Δ(3,3,3) represents the glycoform percentage of an internal Δ-unsaturated hexasaccharide, Δ(4,4,4) represents the glycoform percentage of an internal Δ-unsaturated octasaccharides. A representative tandem mass spectrum of (2,2,2) is shown in supplemental Figure 2.

Tissue Sample		CSA-like GlcAGalNAc4S	CSB-like IdoAGalNAc4S	CSC-like GlcAGalNAc6S
5-μg H-B1 Cartilage	Δ(2,2,2)	4.5 ± 1.2	0.7 ± 0.1	94.9 ± 1.1
	Δ(3,3,3)	5.9 ± 0.4	0.3 ± 0.1	93.8 ± 0.4
	Δ(4,4,4)	7.1 ± 2.2	2.3 ± 1.8	90.6 ± 1.6
5-μg JB-B3 Cartilage	Δ(2,2,2)	40.8 ± 2.7	1.4 ± 0.3	57.8 ± 2.6
	Δ(3,3,3)	42.0 ± 1.1	1.0 ± 0.3	57.0 ± 0.8
	Δ(4,4,4)	43.8 ± 1.7	0.9 ± 0.8	55.3 ± 2.1
5-μg JB-Ligament	Δ(2,2,2)	2.3 ± 1.1	43.2 ± 1.6	54.5 ± 0.4
	Δ(3,3,3)	2.3 ± 0.2	42.4 ± 0.3	55.3 ± 0.3
	Δ(4,4,4)	2.7 ± 0.4	44.2 ± 0.9	53.1 ± 0.5
5-μg JB-Muscle	Δ(2,2,2)	2.5 ± 1.4	58.8 ± 2.9	38.6± 1.6
	Δ(3,3,3)	3.6 ± 0.8	58.2 ± 0.5	38.1 ± 0.6
	Δ(4,4,4)	NA	NA	NA
5-μg JB-Tendon	Δ(2,2,2)	4.4 ± 1.4	42.7 ± 1.3	52.8 ± 0.5
	Δ(3,3,3)	4.2 ± 0.8	44.5 ± 0.8	51.3 ± 0.7
	Δ(4,4,4)	4.0 ± 1.3	43.9 ± 0.2	52.2 ± 1.1
5-μg JB-Synovium	Δ(2,2,2)	47.2 ± 0.7	1.4 ± 0.2	51.4 ± 0.8
	Δ(3,3,3)	45.8 ± 0.4	1.2 ± 0.3	53.1 ± 0.4
	Δ(4,4,4)	47.1 ± 0.1	0.6 ± 0.2	52.3 ± 0.4